Journal of Data Acquisition and Processing
ISSN: 1004-9037
https://sjcjycl.cn/
DOI: 10.5281/zenodo.7766156

FEATURE EXTRACTION AND PREPROCESSING OF DIABETIC RETINAL FUNDUS IMAGES FOR EARLY DETECTION OF DIABETIC RETINOPATHY

K. Kaushika[1], S. Santhosh Baboo[2]
[1]Research Scholar, [2]Principal & Research Supervisor
PG & Research Department of Computer Science and Applications[1,2]
[1,2]Dwaraka Doss Goverdhan Doss Vaishnav College (Autonomous), Chennai, Tamilnadu, India, *[1]kausikak@gmail.com, [2]Santhos1968@gmail.com*

Abstract: According to a review of clinical reports, more than 10% of diabetic individuals have a significant chance of developing eye problems. Eighty to eighty-five percent of people with diabetes who have had the disease for longer than ten years will develop diabetic retinopathy (DR), an eye condition. In clinics, diabetic retinopathy disease is frequently seen and assessed using retinal fundus imaging. Machine learning algorithms have a very difficult time processing the raw retinal fundus images. This study uses image enhancing, resizing, histogram equalisation, and green channel extraction to perform pre-processing on raw retinal fundus images. Moreover, fourteen features are extracted for quantitative analysis from pre-processed photos. The experiments are carried out using the Kaggle dataset for diabetic retinopathy, and the outcomes are assessed by taking into account the mean value and standard deviation for the characteristics that were retrieved.

Keywords: Diabetic retinopathy; Image processing, Retinal fundus images; Median Filter; Feature selection; Feature extraction

I. INTRODUCTION

The number of diabetic people who have diabetic retinopathy has dramatically increased in recent years (DR). One of the most common chronic disorders, DR is the primary factor in middle-aged vision loss in the developed world [1]. Small alterations in the retinal capillaries signal the emergence of DR. Microaneurysms, which are localised interruptions of the retinal capillary, are the first differentiable deviations. Intraregional bleeding is produced by the deformed microaneurysms. This causes the first stage of DR, also known as moderate non-proliferative diabetic retinopathy [2], to develop. Fundus imaging is more suited for noninvasive types of screening since the eye fundus is sensitive to some vascular disorders. The quality and precision of the fundus image extraction technique together with effective image processing methodologies [3] for recognising the abnormalities [4, 5] strongly influence the screening approach's outcome.

Exudates are merely greasy deposits that leak from the damaged ends of blood vessels. The DR is known as moderate nonproliferative diabetic retinopathy once it begins to manifest. Diabetic maculopathy is the term for when these exudates begin to appear around the area of the central vision. The microinfarcts in the retina eventually block the blood vessels as the retinopathy worsens over time. Soft exudates are the medical name for these little infarcts.

When all three of the aforementioned anomalies are present, the retinopathy is referred to as severe non-proliferative diabetic retinopathy [6]. Fluorescein angiography, direct and indirect ophthalmoscopy, stereoscopic colour film fundus photography, and mydriatic or non-mydriatic digital colour or monochromatic photography are just a few of the methods that have been utilised to detect and characterise DR. Direct ophthalmoscope performed by non-ophthalmologists has a sensitivity of about 50% for the diagnosis of proliferative retinopathy under normal clinical circumstances [7, 8].

II. REVIEW OF LITERATURE

According to the analysis of the papers, almost two-fifths of those who self-identify as having DM9 are affected by diabetic retinopathy. By employing an ophthalmoscope screening tool to examine the eye structures of normal and diabetic patients, Harding et al. were the first to identify diabetic retinopathy. The results were 97 and 73%, respectively, in terms of specificity and sensitivity [5]. The optic disc, the fovea, and the blood vessels were among the typical elements of the fundus images. Exudates and blot haemorrhages were among diabetic retinopathy's primary aberrant characteristics [6].

Exudates were originally detected and identified by Philips et al. For exudate identification, three strategies — thresholding, edge detection, and classification—were used. To segment exudate lesions, global and local thresholding values were employed. Calculated values for sensitivity and specificity were 100% and 71%, respectively [10]. The ability to detect retinopathy is one of single-field fundus photography's key benefits, according to professional readers. Its specificity ranges from 85 to 97 percent, and its sensitivity ranges from 61% to 90% [11]. In order to retrieve the optical disc boundary, the red and green channels are used. In 99% of instances, the location methodology was successful. Automated segmentations and genuine OD areas were produced by the segmentation algorithm in 86% [12].

In their innovative methodology for optic disc detection, Ravishankar et al. first identified the major blood arteries and then used their bifurcation to determine the optic disk's approximate position. Many classifiers, such as fuzzy C-means clustering, SVM, neural networks, PCA, and straightforward Bayesian classification [13], have been evaluated. Back propagation neural networks were employed by GG Gardener and colleagues. Exudates area, blood vessel area, haemorrhages area, edoema, and microaneurysms area were the features chosen for the detection. One hundred forty-seven patients with DR and thirty healthy individuals' retinal pictures with exudates, retina with haemorrhages or microaneurysms, retina with blood vessels and without blood vessels were examined.

The outcome revealed that the specificity and sensitivity values were, respectively, 88.4 and 83.5 [14]. By immediately detecting the blood vessels and hard exudates, Mookiah et al. developed a new methodology for the totally automatic classification of all retinal fundus images into several classifications. The key factors considered were area, Shannon entropy, Kapur entropy, and the point where two blood veins split. They applied the Local Binary Pattern idea to extract textual information (LBP). It was noted that SVM with a linear kernel achieved an accuracy of 77.56% whereas C4.5, a form of decision tree, achieved an accuracy of 88.46%. A specificity and sensitivity value of 95.7 and 94.2, respectively, were also revealed

by the results. For low-quality images, Akara et al. suggested an exudate detection approach based on mathematical morphology on retinal images of pupils that are not dilated [15].

The tightly distributed cluster of exudates' primary properties were revealed by the stimulus' standard deviation, which was acquired as a result of the preprocessing step's local variation operator. Exudate detection was reported to have a sensitivity and specificity value of 80% and 99.5%, respectively [16]. The three main challenges in MA detection, including non-uniform illumination and interference from related objects, were addressed by Xiaohui et al. with the SVM classifier, the KPCA produced a superior result than PCA. KPCA successfully obtained 90.6% true positives [17] when there are 2 FP left on each image. Judah et al. segmented the image using the retrieved feature and applied SVM and KNN classifiers to categorise the image based on its severity grade [18].

A segmentation method based on effective course to fine segmentation utilising fuzzy c-means (FCM) clustering and colour representation in Luvs colour space was proposed by Alireza et al. They utilised retinal colour information to help us achieve our goals and demonstrated the improvement brought about by gray-level-based methods. An accuracy of 85.6%, sensitivity of 97.2, and specificity of 85.4 [10] were obtained from the FCM clustering.

In this study, describe the processes for extracting features from retinal fundus images and feature ranking. Moreover, exudate removal, optic disc removal, contrast enhancement, green channel and MA extraction, and haemorrhage detection are covered in this work.

III. MATERIALS AND METHODS

Figure 1 shows the methodology's process flow that was used to carry out the current investigation. The pre-processing of retinal fundus pictures for the extraction and ranking of useful features in the identification of diabetic retinopathy is described in the following subsections.

A. Data Acquisition Phase

The Kaggle platform offers a sizable collection of high-resolution fundus photos obtained in a range of imaging settings. On a scale of 0 to 4, a clinician (trained pathologist) graded the data set for the presence of diabetic retinopathy in each image using the following scale: 0 - No DR, 1 – Mild, 2 – Moderate, 3 – Severe, 4 - Proliferative DR.

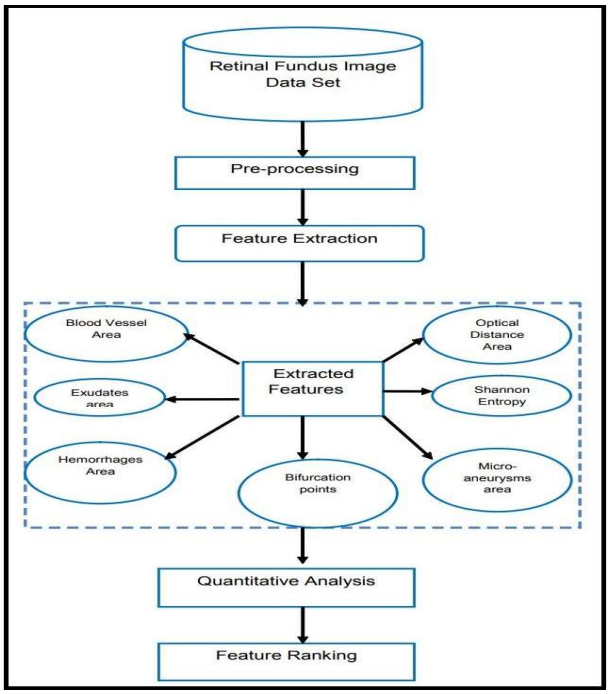

Figure 1: Process Flow for Feature Ranking Retinal Fundus Images

The images were captured using a wide range of different camera models and configurations. As a result, some of the photographs can be blurry or dark. The data set consists of 30 images of diabetic retinopathy and 30 images of normal retinopathy for quantitative analysis. This data collection assists in determining the specific values of the attributes taken into account [19]. As stated in the literature study section, this work took into account 14 features that were gathered from diverse sources. Table 1 [20] lists the factors that were taken into account.

B. Feature selection

Throughout the feature selection process, the characteristics in data that contribute the most to the output or prediction variable that interests are automatically chosen. The Optic distance, Fovea, Blood vessel, Blot hemorrhages, Exudate number, Edema, Bifurcation between two blood vessel, Shannon entropy, Kapur entropy, Renyi's entropy, LBP entropy, LBP energy, Microaneurysm, Exudates Area are the extracted features from retinal fundus images, Feature selection can be used to identify and remove unnecessary, irrelevant, and redundant attributes from data that do not improve the classifier's accuracy or occasionally have a tendency to make the model less accurate. Here, selected 7 traits out of a total of 14 to take into account for the experiment.

C. Pre-processing

Preprocessing, segmentation, and feature ranking are the processes used to find diabetic retinopathy. To guarantee that the dataset is consistent and only shows features that are pertinent, preprocessing is necessary. To reduce the workload of the processes that follow, this

step is important. The photos are then divided into segments to distinguish between normal and pathological chemicals.

Green Channel of the three color channels in the image (Red, Green, and Blue) the contrast between the blood vessels, exudates, and haemorrhages is best observed in the green channel, which is neither under-illuminated nor over-saturated like the other two. For analysis and classification, we have just taken the green channel, which is shown in Figure 2 as an example.

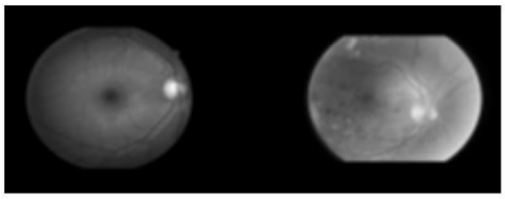

Figure 2: Separation of green channel of images

Contrast Enhancement uses contrast limiting adaptive histogram equalisation to accentuate the image's elements even more. The histogram is equalised, and the image is divided into smaller chunks [29].

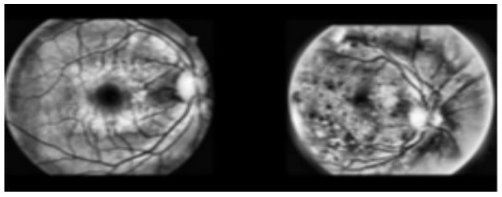

Figure 3: Images after contrast enhancement and cropping to field of view

Resizing and cropping these had to be standardised because the original photographs' sizes varied greatly and some were cropped at the top and bottom. So the circular field of vision (FOV) of an image—the portion of the retina visible in the image—must first be cropped to a square with a side equal to the FOV's diameter. While some photos lack the top and bottom portions, the images that do are uniformed by adding a back patch. Then, as seen in Figure 3, the new square picture is downscaled to 214 X 214 pixels.

D. Feature Extraction

Exudate detection and Optic Disk Removal the removal of the optic disc prior to the start of the process is the primary goal of exudate detection. Because it appears with a similar intensity, hue, and contrast to the other elements of the fundus image, it is crucial. The presence of high contrast circular form portions allows one to distinguish the optic disc from other objects. It should be emphasised that vessels exhibit strong contrast as well. They are noticeably less numerous and smaller in size. It is possible to eliminate the blood vessel that is located inside the optic disc region by using the grayscale closing operator (ö). A flat disc-shaped element with a constant radius of (B1) is employed to achieve this goal, as demonstrated in Eq (1).

$$OP1 = f(B1)\ (fI) \quad ...(1)$$

Where, B1 is the morphological structuring element

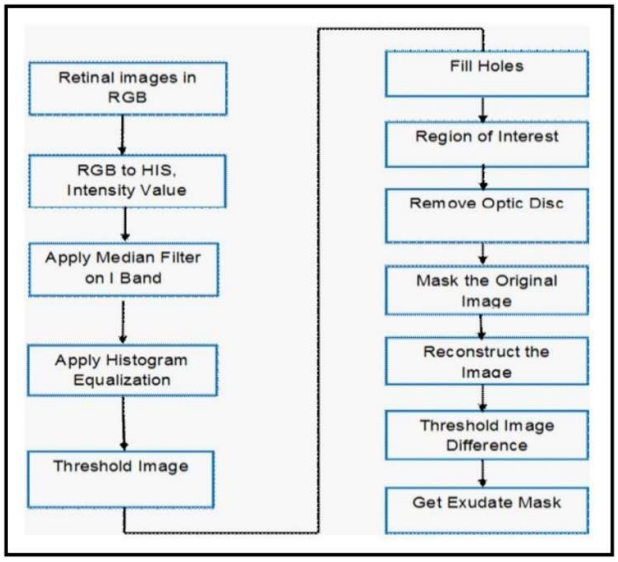

Figure 4: Steps for Exudate Elimination

Exudates to remove the area of low intensity from the final image, a threshold at automatically chosen grey levels was applied. A flat disc structural element with a constant radius of 6(B1) [15] is used to make sure that all the surrounding pixels of the threshold result were added in the chosen region. Exudates elimination processes are given in Figure 4 and an example of eliminating optical discs is provided in Figure 5.

Figure 5: Optic Disc Elimination

Hemorrhages and Microaneurysms A classification process is used in the identification of haemorrhages and microaneurysms. Preprocessing is done after obtaining the data from Messidor utilising the picture segmentation method.

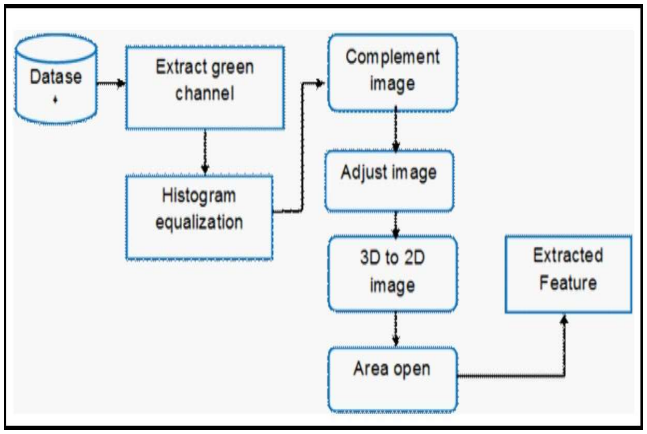

Figure 6: Steps for Microaneurysms and Hemorrhages Detection

Following that, the image is chosen and classified using the ResNet classifier [32]. Both the filter and the wrapper class are utilised in the selection process. Hemorrhages and microaneurysms are identified from the data and plotted in the graph as shown [33].

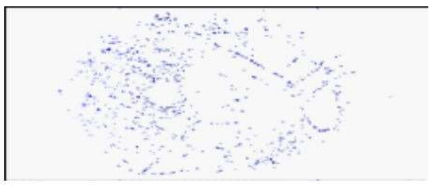

Figure 7: Microaneurysms

Figure 6 depicts the procedures for detecting microaneurysms and haemorrhages, while Figures 7 and 8 exhibit examples of microaneurysms and haemorrhages, respectively.

Figure 8: Hemorrhages

Vascular system Thus may infer that the blood vessels within the OD operate as significant deviators by examining the gray-level picture from the red or green field of the sub-image including the OD (Fig. 3, images R and G). As a result, they should be removed from the image beforehand. Because the vasculature is piecewise straight and linear, it can be envisioned as a structure made up of numerous connected linear shapes that are comparable in length and width.

These linear structures were typically created by a group of pixels with nearly constant grey levels and values that were somewhat lower than the surrounding non-vessel pixels' grey levels. You may determine a linear shape by computing the statistical variance of the gray-level values of the pixels that are connected with it using a rotating linear structuring element with length and width both set to one. In contrast, the rotation with the highest value will refer to the circumstance in which the linear shape [34] crosses. The rotation associated with the lowest value will be that in which the vessel comprises.

IV. RESULTS AND DISCUSSION

A different set of feature values for photographs of the normal retinal fundus and images of the retina damaged by diabetes is used for the experiments. 30 images of each category had the feature values calculated using the Python digital image processing (DIP) packages. Table 3 summarises the mean and standard deviation values that were taken from retinal fundus pictures of both healthy and diabetic individuals.

Table 1: Standard Range for Values of Various Features

Features	Normal	Diabetic Retinopathy
Exudate area	0.00	1015.23
Blood Vessel area	37230.56	33545.54
Bifurcation point count	305.40	309.65
Shannon entropy	6.35	6.04

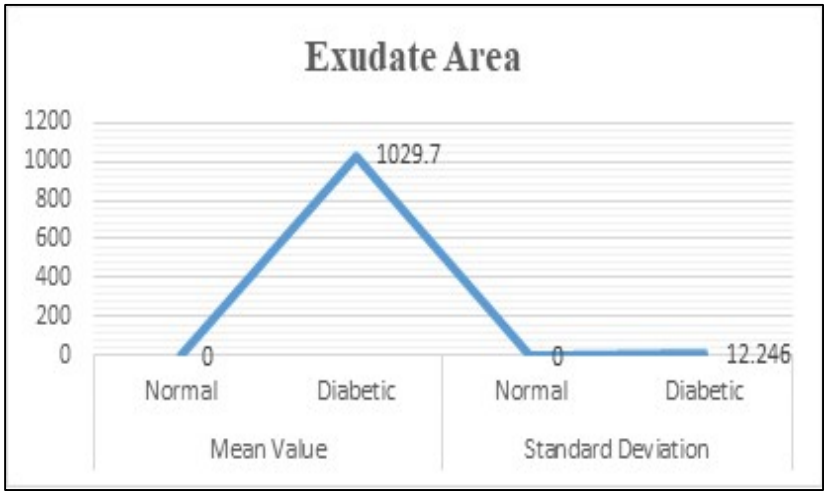

Figure 9: Comparison of exudate area for normal and diabetic retinal images

As can be seen from Table 2, exudates, haemorrhage, and MA values all decrease to zero when compared to normal retinal pictures. Based on the feature rating criteria, the mean difference between each image was calculated. Table 1 displays the typical range for each of the distinct traits.

Table 2: Mean and SD of 7 features for Normal and Diabetic Retinal Images

Features	Mean Value		Standard Deviation	
	Normal	Diabetic	Normal	Diabetic
Exudate Area	0.00	1029.70	0.00	12.24
Blood Vessel area	38486.79	34672.62	2839.39	2311.86
Bifurcation point count	332.24	315.08	20.12	12.34
Shannon entropy	6.50	5.85	0.22	0.08
Optic Distance	928.80	925.36	10.74	19.35
Hemorrhage area	79323.40	90642.15	28384.45	390000.00

MA area	86188.00	63435.00	23626.00	23759.00

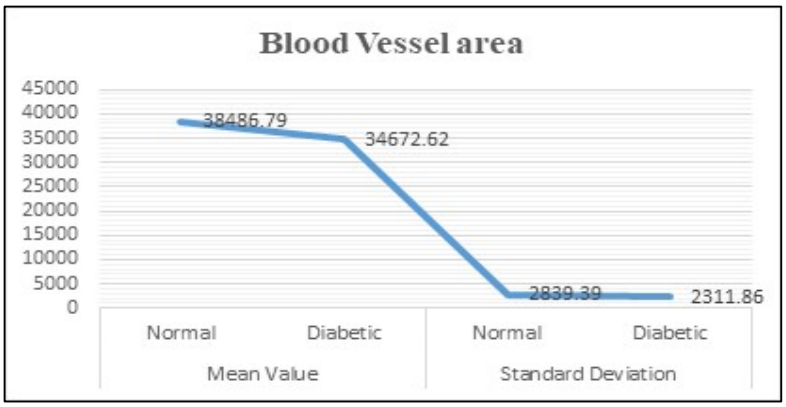

Figure 10: Comparison of bifurcation point count for normal and diabetic retinal images

According to Figure 9, the exudate area's mean value and standard deviation for a normal retinal picture are 0 and for a diabetic retinal image, 1029.7 and 12.246 respectively. Similar to Figure 9, the bifurcation point count in Figure 10 reveals that the mean and standard deviation of normal retinal images are 332.245 and 20.120, respectively, and that they are 315.09 and 12.34, respectively, for diabetic retinal images.

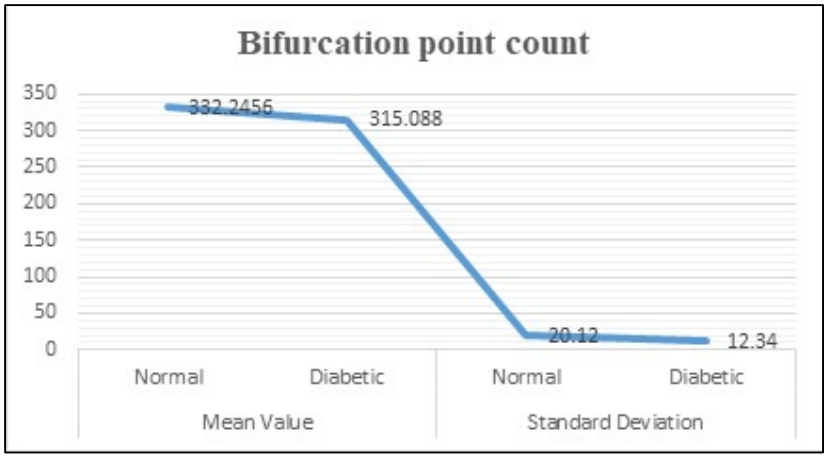

Figure 11: Comparison of blood vessel area for normal and diabetic retinal images

As shown in Figure 11, the mean value and standard deviation of the blood vessel area for normal retinal images are 34673 and 2311.86, respectively, while they are 38352.60 and 2839.39, respectively, for diabetes retinal images.

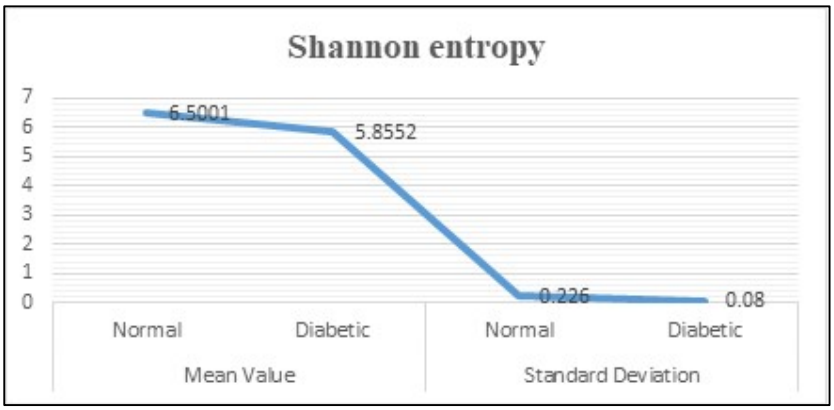

Figure 12: Comparison of Shannon entropy for normal and diabetic retinal images

Figure 12 shows that the Shannon entropy for typical retinal pictures has a mean value of 6.5001 and a standard deviation of 0.226. The Shannon entropy of diabetic retinal pictures has a mean of 5.855 and a standard deviation of 0.08, which we can again infer from the same graphic.

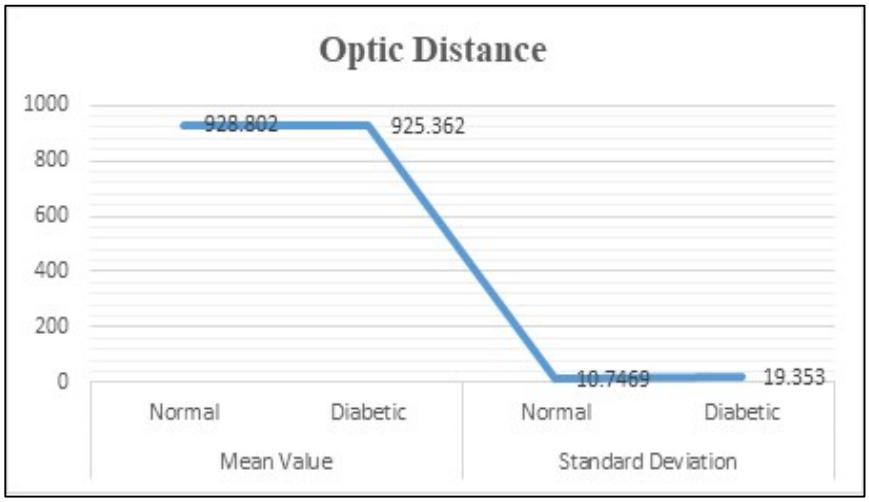

Figure 13: Comparison of optic distance for normal and diabetic retinal images

The optic distance for normal retinal pictures has a mean value of 928.80 and a standard deviation of 10, as shown in Figure 13. The mean and standard deviation values for an optic distance of diabetic retinal pictures are 925.36 and 19.353 correspondingly, according to the same figure.

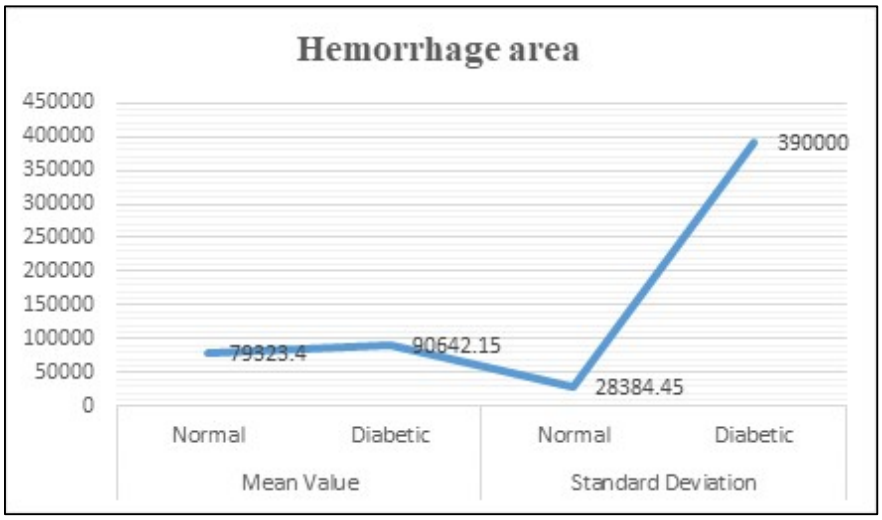

Figure 14: Comparison of hemorrhage for normal and diabetic retinal images

Figure 14 makes it clear that the hemorrhage's mean value and standard deviation for retinal photographs taken under normal circumstances are 79323.4 and 28384.45, respectively. The mean and standard deviation values for an MA of diabetic retinal pictures are 90642.15 and 390000, respectively, according to the same figure.

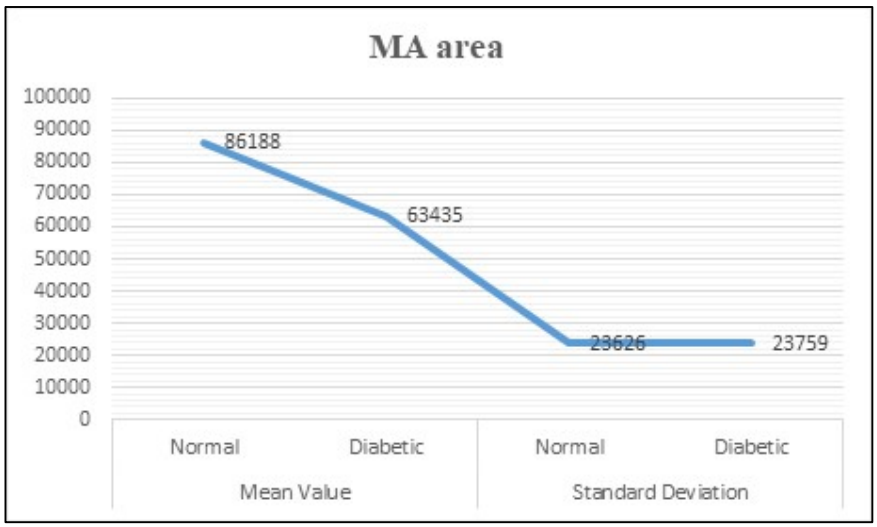

Figure 15: Comparison of MA for normal and diabetic retinal images

The average value and standard deviation of the MA for the typical retinal pictures in Figure 15 are 86188 and 23626, respectively. The mean and standard deviation values for an MA of diabetic retinal pictures are 63435 and 23759, respectively, according to the same figure.

From the aforementioned study, may infer that exudates, which are completely absent from typical retinal pictures, are the highest ranking feature, followed by blood vessels, which have the biggest mean difference. The approach described in [2] has also been used to calculate the absolute mean difference. The performance of diabetic retinopathy detection systems may be enhanced by further examination of the exudates region and micro characteristics retrieved from the exudates area.

V. CONCLUSION

In this study, machine learning approaches are used to pre-process and extract features from the diabetic retinal fundus image in order to detect diabetic retinopathy. Using the DIP toolbox of Python packages, pre-processing techniques like green channel extraction, histogram equalisation, and scaling were carried out. The photos were split into two separate datasets: one contained photographs of retinas damaged by diabetes, and the other had images of a normal stimuli. From normal and diabetic retinal fundus imaging data sets, the total of 14 physiologically relevant features are retrieved. Seven of the most important features out of all the retrieved data are used for comparison; rating these features is relatively straightforward and essential for distinguishing between a normal and diabetic fundus image. According to the results, the exudate area, followed by blood vessels and other features, is the feature that may be most effectively utilised to detect diabetes. This shows that exudate is one of the main features that cause diabetic retinopathy. Due to their biological significance and prior outcomes, the features considered in this investigation are particular. Future aspects can be derived from properties including edoema, red lesions, Kapoor entropy, and other characteristics. It can be used to classify images of diabetic retinopathy into various categories depending on the values of the features, and performance may be assessed using various metrics.

REFERENCES

[1] N. B. Prakash and D. Selvathi, “An Efficient Detection System for Screening Glaucoma in Retinal Images”, *Biomed. Pharmacol. Jorurnal*, Vol. 10(1), 2017.

[2] S. S. Rathore and A. Gupta, “A comparative study of feature-ranking and feature-subset selection techniques for improved fault prediction”, *Proceedings of the 7th India Software Engineering Conference on - ISEC ’14*, pp. 1–10, 2014.

[3] S. Sisodia and S. Verma, “Image pixel intensity and artificial neural network based method for pattern recognition”, *World Acad. Sci. Eng. Technology*, pp. 742–745, 2011.

[4] M. Merlin and B. Priestly Shan, “Robust and efficient segmentation of blood vessel in retinal images using gray-level textures features and fuzzy SVM”, *Biomed. Pharmacol. Journal*, Vol. 8(2), pp. 1111–1120, 2015.

[5] T. Kauppi, V. Kalesnykiene, J.-K. Kamarainen, L. Lensu, I. Sorri, A. Raninen, R. Voutilainen, H. Uusitalo, H. Kalviainen, and J. Pietila, “The DIARETDB1 Diabetic retinopathy database and evaluation protocol”, *Proceedings of the British Machine Vision Conference*, pp. 15.1-15.10, 2007.

[6] Sopharak, B. Uyyanonvara, and S. Barman, “Automatic exudate detection from non-dilated diabetic retinopathy retinal images using Fuzzy C-means clustering”, *Sensors*, Vol. 9(3), pp. 2148–2161, 2009.

[7] S. K. and D. M. and D. Santhi, “Effective Segmentation of Optic Disc in Retinal images for diagnosing Eye Diseases that leads to Blindness”, *Biomedical Pharmacol. Journal*, Vol. 8(1), pp. 427–434, 2015.

[8] S. P. Harding, D. M. Broadbent, C. Neoh, M. C. White, and J. Vora, “Sensitivity and specificity of photography and direct ophthalmoscopy in screening for sight threatening eye disease: the Liverpool Diabetic Eye Study”, *BMJ*, Vol. 311(7013), pp. 1131–5, 1995.

[9] M. N. Langroudi and Hamed Sadjedi, "A New Method for Automatic Detection and Diagnosis of Retinopathy Diseases in Colour Fundus Images Based on Morphology", *International Conference on Bioinformatics and Biomedical Technology*, pp. 134–138, 2010.

[10] Osareh, B. Shadgar, and R. Markham, "A computational-intelligence-based approach for detection of exudates in diabetic retinopathy images", *IEEE Trans. Inf. Technol. Biomed.*, Vol. 13(4), pp. 535–545, 2009.

[11] A. Williams, I. U. Scott, J. A. Haller, A. M. Maguire, D. Marcus, and H. R. McDonald, "Single-field fundus photography for diabetic retinopathy screening: A report by the American Academy of Ophthalmology", *Ophthalmology*, Vol. 111(5), pp. 1055–1062, 2004.

[12] U. Morphological, E. Detection, A. Aquino, M. E. Gegúndez-arias, and D. Marín, "Detecting the Optic Disc Boundary in Digital Fundus Feature Extraction Techniques", Vol. 29(11), pp. 1860–1869, 2010.

[13] S. Ravishankar, A. Jain, and A. Mittal, "Automated feature extraction for early detection of diabetic retinopathy in fundus images", *Computer Vision and Pattern*, pp. 210–217, 2009.

[14] T. H. Williamson, "Automatic detection of diabetic retinopathy exudates from non-dilated retinal images using mathematical ... retinal images using mathematical morphology methods", *Comput. Med. Imaging Graph.*, Vol. 32(8), pp. 720–727, November 2016.

[15] Sopharak, B. Uyyanonvara, S. Barman, and T. H. Williamson, "Automatic detection of diabetic retinopathy exudates from non-dilated retinal images using mathematical morphology methods", *Comput. Med. Imaging Graph*., Vol. 32(8), pp. 720–727 ,2008.

[16] M. Niemeijer, B. Van Ginneken, S. R. Russell, M. S. A. Suttorp-Schulten, and M. D. Abràmoff, "Automated detection and differentiation of drusen, exudates, and cotton-wool spots in digital color fundus photographs for diabetic retinopathy diagnosis", *Investig. Ophthalmol. Vis. Sci*., Vol. 48(5), pp. 2260–2267, 2007.

[17] X. Zhang and O. Chutatape, "Top-down and Bottom-up Strategies in Lesion Detection of Background Diabetic Retinopathy", *Top-down and Bottom-up Strategies in Lesion Detection of Background Diabetic Retinopathy*, pp. 422–428, 2005.

[18] Lachure, A. V. Deorankar, S. Lachure, S. Gupta, and R. Jadhav, "Diabetic Retinopathy using morphological operations and machine learning", *Souvenir of the 2015 IEEE International Advance Computing Conference*, pp. 617–622, 2015.

[19] "Kaggle Diabetic Retinopathy Detection," 2015. [Online]. *Available: https://www.kaggle.com/c/diabetic-retinopathy-detection.*

[20] M. R. K. Mookiah, U. R. Acharya, R. J. Martis, C. K. Chua, C. M. Lim, E. Y. K. Ng, and A. Laude, "Evolutionary algorithm based classifier parameter tuning for automatic diabetic retinopathy grading: A hybrid feature extraction approach", *Knowledge-Based Systems*, Vol. 39, pp. 9–22, 2013.

[21] Minar, J., Pinkava, M., Riha, K., Dutta, M. K., & Sengar, N, "Automatic extraction of blood vessels and veins using laplace operator in fundus image", *International Conference on Green Computing and Internet of Things (ICGCIoT)*, pp. 23-26.

[22] Thanapong, C., Watcharachai, W., & Somporn, R, "Extraction blood vessels from retinal fundus image based on fuzzy C- median clustering algorithm", *IEEE Fourth International Conference on Fuzzy Systems and Knowledge Discovery*, Vol. 2, pp. 144-148, 2007.

[23] Elbalaoui, A., Fakir, M., Taifi, K., & Merbouha, A, "Automatic Detection of Blood Vessel in Retinal Images", *IEEE 13th International conference on Computer Graphics, Imaging and Visualization (CGiV)*, pp. 324-332, March, 2016.

[24] Bansal, A., Vats, A., Jain, A., Dutta, M. K., Burget, R., & Prinosil, J, "An efficient automatic intensity based method for detection of macula in retinal images", *IEEE 39th International Conference on Telecommunications and Signal Processing (TSP),* pp. 507-510, 2016, June.

[25] Lin, "Divergence measures based on the Shannon entropy", *IEEE Trans. Inf. theory*, Vol. 37(1), pp. 145–151, 1991.

[26] Kaufman, U. Zurcher, and P. S. Sung, "Entropy of electromyography time series", *Phys. A Stat. Mech. its Appl.*, Vol. 386(2), pp. 698–707, 2007.

[27] R. Szeliski, R. Zabih, D. Scharstein, O. Veksler, V. Kolmogorov, A. Agarwala, M. Tappen, and C. Rother, "A Comparative Study of Energy Minimization Methods for Markov Random", *Part II LNCS*, Vol. 3952, pp. 16–29, 2006.

[28] Niemeijer, B. Van Ginneken, M. J. Cree, S. Member, A. Mizutani, B. Zhang, R. H. Member, M. Lamard, C. Muramatsu, X. Wu, G. C. Member, J. You, Q. Li, Y. Hatanaka, C. Roux, and F. Karray, "Retinopathy Online Challenge: Automatic Detection of Microaneurysms in Digital Color Fundus Photographs", Vol. 1, pp. 185–195, 2010.

[29] T. Walter, J.-C. Klein, P. Massin, and A. Erginay, "A contribution of image processing to the diagnosis of diabetic retinopathy—detection of exudates in color fundus images of the human retina", *IEEE Trans. Med. Imaging*, Vol. 21(10), pp. 1236–1243, 2002.

[30] Minar, J., Riha, K., Krupka, A., & Tong, H, "Automatic detection of the macula in retinal fundus images using multilevel thresholding", *International Journal of Advances in Telecommunications, Electrotechnics, Signals and Systems*, Vol. 3(1), pp. 13- 16, 2016.

[31] C. Sinthanayothin, J. F. Boyce, T. H. Williamson, H. L. Cook, E. Mensah, S. Lal, and D. Usher, "Automated detection of diabetic retinopathy on digital fundus images" *Diabet. Med.*, Vol. 19(2), pp. 105–112, 2002.

[32] S. Gupta and R. Jadhav, "Diabetic Retinopathy using Morphological Operations and Machine Learning", *IEEE International Conference on Advance Computing*, pp. 617–622 2015.

[33] U. Akram, S. Khalid, and S. A. Khan, "Identification and classification of microaneurysms for early detection of diabetic retinopathy", *Pattern Recognition*, Vol. 46(1), pp. 107–116, 2013.

[34] D. Marín, A. Aquino, M. E. Gegúndez-Arias, and J. M. Bravo, "A new supervised method for blood vessel segmentation in retinal images by using gray-level and moment invariants-based feature", *IEEE Trans. Medical Imaging*, Vol. 30(1), pp. 146–158, 2011.

[35] Hann, Christopher E., James A. Revie, Darren Hewett, J. Geoffrey Chase, and Geoffrey M. Shaw, "Screening for diabetic retinopathy using computer vision and physiological markers", *Journal of diabetes science and technology*, Vol. 4, pp. 819-834, 2009.

[36] B. Harangi, I. Lazar and A. Hajdu, "Automatic Exudate Detection Using Active Contour Model and Region wise Classification", *IEEE EMBS*, pp.5951–5954, 2012.

[37] Balazs Harangi, Balint Antal and Andras Hajdu, "Automatic Exudate Detection with Improved Nave-Bayes Classifier, Computer-Based Medical Systems", *CBMS*, pp. 1–4, 2012.

[38] Ram K, and Sivaswamy J, "Multi-space clustering for segmentation of exudates in retinal color photographs", *IEEE Engineering in Medicine and Biology Society (EMBC 09)*, pp. 1437-1440, 2009.

[39] T. Walter, J.C. Klein, P. Massin and A. Erginay, "A contribution of image processing to the diagnosis of diabetic retinopathy detection of exudates in color fundus images of the human retina", *IEEE Transactions on Medical Imaging*, Vol. 21(10) 2002.

[40] Sopharak, Bunyarit Uyyanonvara, Sarah Barman and Thomas H.Williamsonc, "Automatic detection of diabetic retinopathy exudates from nondilated retinal images using mathematical morphology methods", *Computerized Medical Imaging and Graphics*, pp. 720– 727, 2008.